# A novel renal carbonic anhydrase type III plays a role in proximal tubule dysfunction

P Gailly[1,10], F Jouret[2,10], D Martin[1], H Debaix[2], KS Parreira[2], T Nishita[3], A Blanchard[4], C Antignac[5], TE Willnow[6], PJ Courtoy[7], SJ Scheinman[8], EI Christensen[9] and O Devuyst[2]

[1]Division of Cell Physiology, Christian de Duve Institute of Cellular Pathology, Université catholique de Louvain, Brussels, Belgium; [2]Division of Nephrology, Christian de Duve Institute of Cellular Pathology, Université catholique de Louvain, Brussels, Belgium; [3]Laboratory of Veterinary Physiology, Azabu University, Sagamihara-Shi, Japan; [4]Centre d'Investigations Cliniques, Hôpital Européen Georges Pompidou, Paris, France; [5]Inserm U574 and Department of Genetics, Necker Hospital, Paris, France; [6]Max Delbrueck Center for Molecular Medicine, Berlin, Germany; [7]Cell Unit, Christian de Duve Institute of Cellular Pathology, Université catholique de Louvain, Brussels, Belgium; [8]Department of Medicine, SUNY Upstate Medical University, Syracuse, New York, USA and [9]Department of Cell Biology, Institute of Anatomy, University of Aarhus, Aarhus, Denmark

Dysfunction of the proximal tubule (PT) is associated with variable degrees of solute wasting and low-molecular-weight proteinuria. We measured metabolic consequences and adaptation mechanisms in a model of inherited PT disorders using PT cells of ClC-5-deficient (Clcn5Y/−) mice, a well-established model of Dent's disease. Compared to cells taken from control mice, those from the mutant mice had increased expression of markers of proliferation (Ki67, proliferative cell nuclear antigen (PCNA), and cyclin E) and oxidative scavengers (superoxide dismutase I and thioredoxin). Transcriptome and protein analyses showed fourfold induction of type III carbonic anhydrase in a kidney-specific manner in the knockout mice located in scattered PT cells. Kidney-specific carbonic anhydrase type III (CAIII) upregulation was confirmed in other mice lacking the multiligand receptor megalin and in a patient with Dent's disease due to an inactivating CLCN5 mutation. The type III enzyme was specifically detected in the urine of mice lacking ClC-5 or megalin, patients with Dent's disease, and in PT cell lines exposed to oxidative stress. Our study shows that lack of PT ClC-5 in mice and men is associated with CAIII induction, increased cell proliferation, and oxidative stress.

Correspondence: O Devuyst, Division of Nephrology, UCL Medical School, 10 Avenue Hippocrate, B-1200 Brussels, Belgium.
E-mail: Olivier.Devuyst@uclouvain.be

[10]These two authors contributed equally to this work

The epithelial cells lining the proximal tubule (PT) segment of the kidney play an essential role in reabsorbing solutes filtrated by the glomeruli. In particular, PT cells reabsorb albumin and low-molecular-weight (LMW) proteins through an active endocytic pathway that involves two multiligand-binding receptors, megalin and cubilin, which are abundantly expressed at the brush border.[1] Upon ligand binding, the receptors interact and are internalized into coated vesicles, with subsequent delivery to endosomes and lysosomes for ligand processing and receptor recycling. This endocytic trafficking involves the progressive acidification of the endosome–lysosome pathway in PT cells, a process driven by the vacuolar $H^+$-ATPase (V-ATPase) complex.[2]

The generalized dysfunction of the PT, named 'renal Fanconi syndrome,' is associated with variable degrees of solute wasting and LMW proteinuria, which can lead to severe clinical manifestations, such as growth retardation, rickets, nephrocalcinosis, and renal failure. Recent insights into rare inherited disorders show the importance of receptor-mediated endocytosis in the pathophysiology of PT dysfunction. Inactivating mutations in the CLCN5 gene, which encodes the endosomal $Cl^-/H^+$ exchanger ClC-5, are associated with Dent's disease, an X-linked renal Fanconi syndrome associated with hypercalciuria nephrocalcinosis, nephrolithiasis, and renal failure in some patients.[3] ClC-5 is primarily localized in PT cell endosomes, where it co-distributes with the V-ATPase.[4,5] Genetic inactivation of Clcn5 in mice causes renal tubular defects that mimic human Dent's disease, including severe PT dysfunction with impaired endocytosis and trafficking defects of megalin and cubilin leading to LMW proteinuria.[6–8] Similarly, the functional loss of cubilin in Imerslund–Gräsbeck disease[9] or the genetic inactivation of megalin (Lrp2) in mice[10] lead to PT dysfunction with LMW proteinuria.

The biochemical and metabolic outcomes of the PT cell dysfunction associated with inherited renal Fanconi syndrome and the adaptive mechanisms potentially

involved remain poorly understood. Recently, Wilmer *et al.*[11] have reported an increased oxidative stress and altered redox status in PT cells cultured from the urine of patients with cystinosis, a major cause of inherited renal Fanconi syndrome, suggesting that PT dysfunction may be associated with oxidative stress. In this study, we have used *Clcn5* knockout (KO) mice as a well-defined model of Dent's disease and generalized renal Fanconi syndrome[6,7] to investigate the metabolic consequences and adaptive mechanisms of PT dysfunction. The $Clcn5^{Y/-}$ kidneys were characterized by higher cell proliferation and oxidative stress, and the induction of type III carbonic anhydrase (CAIII)—an early mesodermal marker with the lowest hydratase activity of the CA isoforms and no documented role in the kidney.[12] CAIII was exclusively distributed in scattered PT cells and was excreted in $Clcn5^{Y/-}$ urine. These data were confirmed in patients with Dent's disease and investigated in other mouse models of PT dysfunction and PT cell lines exposed to oxidant conditions. Taken together, these observations suggest that generalized PT dysfunction due to the loss of ClC-5 is associated with increased cell proliferation, dedifferentiation, and oxidative stress. Our *in vitro* studies in PT cells support the hypothesis that CAIII production may play a role in response to oxidative damage.

## RESULTS

### Proliferation and oxidative stress in Clcn5$^{Y/-}$ kidneys

Real-time reverse transcription-PCR (RT-PCR) analyses (Figure 1) showed a significant increase in the expression of proliferative cell nuclear antigen (PCNA), Ki67, cyclin E, and osteopontin in the kidneys of $Clcn5^{Y/-}$ mice. Distinct reactive oxygen species scavengers, such as type I superoxide dismutase and thioredoxin, were also upregulated, suggesting the solicitation of cell oxidative defenses in $Clcn5^{Y/-}$ kidneys (Figure 1). These results, obtained in 12–week-old mice, were also observed in 1-year-old $Clcn5^{Y/-}$ mice (data not shown). Immunohistochemistry detected a 3.5-fold increase in the number of PCNA- and Ki67-positive cells in ClC-5-deficient kidneys (∼1.8% of PT cells) vs controls (∼0.5% of PT cells) (Figure 2). Comparative measurement of ethidium fluorescence in kidney sections revealed that the lack of ClC-5 was associated with a major increase in the production of superoxide $O_2^{\bullet-}$ anion in PT cells (Figure 2). These observations showed that the generalized PT dysfunction due to the loss of ClC-5 is reflected by significant cell proliferation and a major oxidative stress that solicitates reactive oxygen species scavengers.

### Comparison of Clcn5$^{Y/+}$ and Clcn5$^{Y/-}$ renal transcriptomes

We next used the amplified fragment length polymorphism (AFLP) procedure to identify genes possibly involved in adaptative mechanisms against PT dysfunction. Using one-third of the possible AFLP primer combinations (see Materials and Methods), a total of 10 cDNA bands were identified as differentially expressed in 12-week-old $Clcn5^{Y/-}$ vs $Clcn5^{Y/+}$ kidneys. One of these bands, significantly
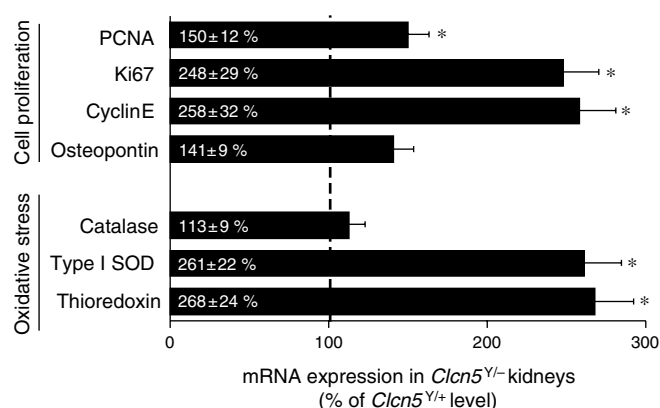


**Figure 1 | Cell proliferation and oxidative stress in ClC-5-deficient kidneys: real-time RT-PCR.** Real-time RT-PCR quantification of mRNA expression of proliferative cell nuclear antigen (PCNA), Ki67, cyclin E, osteopontin, catalase, type I superoxide dismutase (SOD), and thioredoxin in kidneys from $Clcn5^{Y/-}$ vs $Clcn5^{Y/+}$ 12-week-old mice (n = 6 pairs). The mRNA levels were adjusted to GAPDH before quantification and calculated upon the formula: efficiency$^{\Delta\Delta C_t}$. The $Clcn5^{Y/-}$ kidneys show an increased expression of both cell proliferation and oxidative stress markers. Values are presented as mean ratios ± s.d., with $Clcn5^{Y/+}$ level set at 100%; *$P < 0.05$.

upregulated in $Clcn5^{Y/-}$ samples, was identified as a transcript of *Car3* (GenBank accession no. M27796), encoding CAIII. The other cDNA bands, which were differentially expressed in $Clcn5^{Y/-}$ kidneys, corresponded to unidentified mouse contigs. Quantitative real-time RT-PCR was used to validate these results by comparing the mRNA expression of CAIII and CAII, the most abundant CA isoform in the kidney (Figure 3a). The CAIII mRNA expression was approximately fivefold lower than CAII in wild-type kidneys. However, the CAIII transcript was significantly upregulated in ClC-5-deficient kidneys (ratio: 553 ± 48% of $Clcn5^{Y/+}$ level, n = 6), whereas CAII mRNA expression remained unchanged (94 ± 8% of $Clcn5^{Y/+}$ level). A similar induction of CAIII expression was also observed in 1-year-old $Clcn5^{Y/-}$ kidneys, and the results were confirmed on laser capture microdissected cortex samples (data not shown). The upregulation of CAIII mRNA associated with the loss of ClC-5 was specific to the kidney, as CAIII mRNA expression levels in liver, skeletal muscle (vastus lateralis), and lung from $Clcn5^{Y/-}$ mice were unchanged (Figure 3b). These data, obtained using AFLP coupled with real-time RT-PCR, evidenced a significant and kidney-specific induction of *Car3* mRNA expression in mice lacking ClC-5.

### Expression of CAIII in Clcn5 kidney and urine

Affinity-purified anti-CAIII antibodies, with no cross-reactivity for purified CAI and CAII,[13] were used to further investigate CAIII expression in the kidney. These antibodies did not detect any specific signal with *Car3* KO kidney samples, whereas anti-CAII antibodies recognized the appropriate isoform in all samples (Figure 3c). The distinction between CAII and CAIII isoforms was facilitated by their different electrophoretic mobility in 14% sodium dodecyl
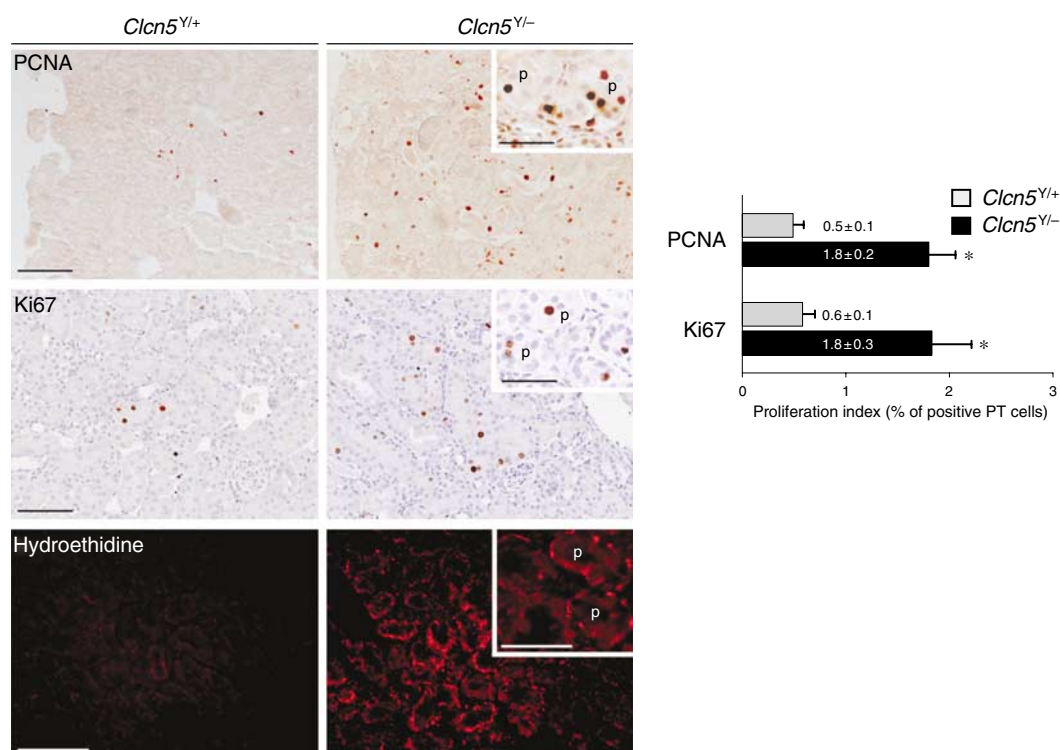
**Figure 2 | Cell proliferation and oxidative stress in ClC-5-deficient kidney: immunostaining and hydroethidine fluorescence.**
Immunostaining for proliferation markers, PCNA and Ki67, and measurement of superoxide anion generation in $Clcn5^{Y/+}$ and $Clcn5^{Y/-}$ kidneys.
Counting of PCNA- and Ki67-positive cells along PT (p) indicates a $\sim$3-fold increase of proliferating PT cells in $Clcn5^{Y/-}$ vs $Clcn5^{Y/+}$ kidneys
($n = 4$ pairs). Values are presented as means ± s.d.; *$P < 0.05$. The detection of red fluorescent ethidium bromide shows a positive signal in
$Clcn5^{Y/-}$ PT (p), in strong contrast to $Clcn5^{Y/+}$ samples ($n = 3$ pairs). Bars = 100 μm (insets, 50 μm).

sulfate-polyacrylamide gel electrophoresis, with CAIII showing a slightly faster migration pattern ($\sim$27 kDa) than CAII ($\sim$29 kDa) (Figure 3d). Using these antibodies, we confirmed the specific, fourfold upregulation of CAIII in ClC-5-deficient kidneys, contrasting with the lack of changes in CAII expression (Figure 3e and f). Similar results were obtained by using a monoclonal antibody against CAIII (data not shown).

Immunoblotting analyses detected a specific excretion of CAIII in urine samples from $Clcn5^{Y/-}$ mice (Figure 4a) and in the urine of three unrelated patients with Dent's disease (Figure 4b). It must be noted that CAIII was detected in simple, non-centrifuged urine samples and that variable levels of CAII could also be detected in such samples, irrespective of the genotype and CAIII levels (data not shown). Thus, CAIII expression is significantly and specifically increased in ClC-5-deficient kidneys, and CAIII is detected in the urine of mice and patients lacking ClC-5.

**Cellular and subcellular distribution of CAIII in mouse kidney**
In normal kidney, a weak immunoreactive signal for CAIII was observed in a subset of PT cells located in the outer cortex, identified by their apical reactivity for the E1 subunit of the V-ATPase (Figure 5a, c, and d). CAIII was detected only in PT cells and not in other cell types, including the α-type IC (Figure 5c and d, arrowheads). In ClC-5-deficient

kidney, the total number of CAIII-positive PT cells in the outer cortex was increased approximately fourfold (17.1 vs 4.2% of $Clcn5^{Y/+}$ PT cells) (Figure 5b). In addition, immunoreactive signal for CAIII was detected in PT of the inner cortex. The number of PT cells undergoing apoptosis established by the TUNEL (terminal uridine deoxynucleotidyl transferase dUTP nick end labeling) reaction was similar in $Clcn5^{Y/+}$ and $Clcn5^{Y/-}$ kidneys (data not shown).

Immunogold analyses showed that in normal kidney cortex, CAIII distribution was mainly cytosolic, also including the apical brush border microvilli (Figure 6a and d). Nuclei were labeled (Figure 6c and f), and a possible endosomal labeling could not be excluded (Figure 6a and d). No significant signal was noticed in mitochondria. In $Clcn5^{Y/-}$ samples, CAIII labeling appeared stronger than in $Clcn5^{Y/+}$ kidneys, with a similar distribution (Figure 6a–c vs d–f). The predominant cytosolic distribution of CAIII, with residual distribution in membrane and nuclear fractions, was confirmed by subcellular fractionation of mouse kidneys, as reported previously in hepatocytes (data not shown).[14] Thus, CAIII is essentially distributed in the cytosol of a subset of PT cells in the outer cortex of normal mouse kidney. The loss of ClC-5 causes a significant increase of CAIII expression in PT cells of both outer and inner cortices, with a similar subcellular localization.
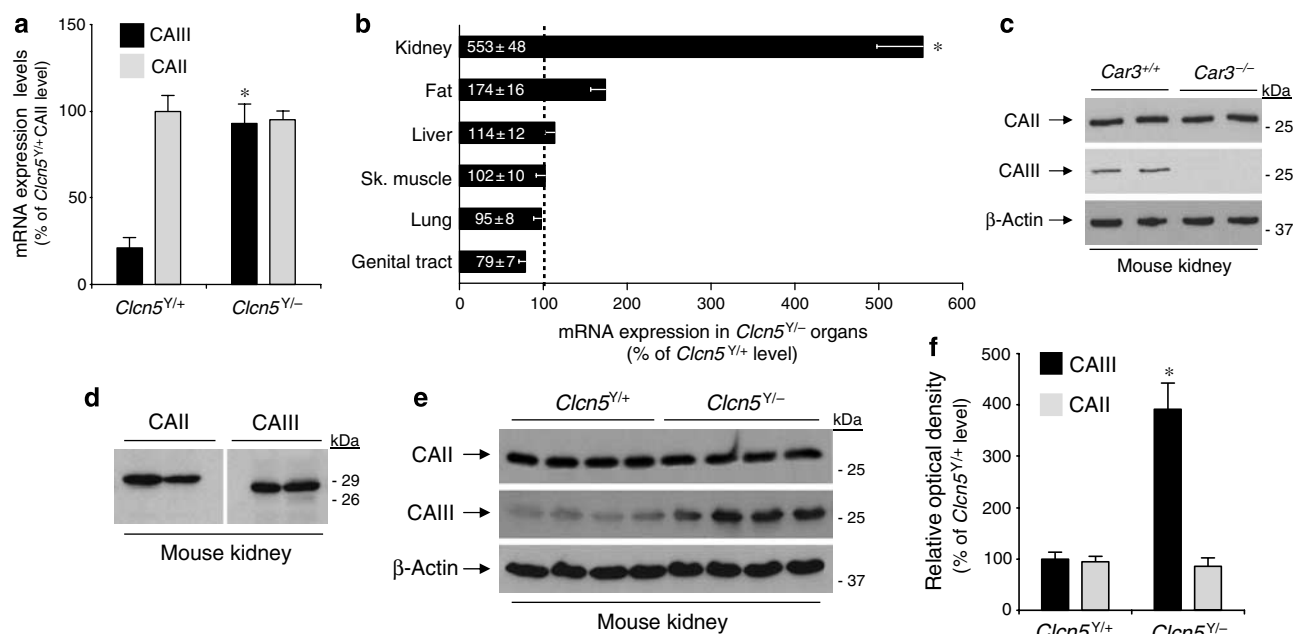
**Figure 3 | Expression of CAIII in *Clcn5*$^{Y/-}$ vs *Clcn5*$^{Y/+}$ kidneys.** (**a**) Real-time RT-PCR quantification of mRNA expression of type III and II CA isozymes in *Clcn5*$^{Y/-}$ vs *Clcn5*$^{Y/+}$ kidneys (*n* = 6 pairs). The mRNA levels were adjusted to GAPDH and then compared between *Clcn5*$^{Y/-}$ and *Clcn5*$^{Y/+}$ samples, using the formula: ratio = $2^{-\Delta\Delta C_t}$.[37] In normal mouse kidneys, CAIII mRNA expression represents ~20% of CAII. By contrast, in *Clcn5*$^{Y/-}$ samples, CAIII expression is ~5 times increased, with no changes in CAII level. (**b**) Real-time RT-PCR quantification of CAIII mRNA expression in *Clcn5*$^{Y/-}$ vs *Clcn5*$^{Y/+}$ kidneys, epididymal fat, liver, skeletal muscle (vastus lateralis), lung, and male genital tract (*n* = 6 pairs). After adjustment of mRNA levels to the reporter gene GAPDH, CAIII mRNA quantification was compared between *Clcn5*$^{Y/-}$ and *Clcn5*$^{Y/+}$ samples, using the formula: ratio = $2^{-\Delta\Delta C_t}$. The induction of CAIII caused by ClC-5 deficiency mostly involves kidneys, with a trend in epididymal fat and no significant changes in other organs. (**c**) Characterization of anti-CAIII antibodies. A portion of 20 μg of cytosolic proteins from total *Car3*$^{+/+}$ and *Car3*$^{-/-}$ kidneys (*n* = 2 pairs of mice) was separated by SDS-PAGE and blotted onto nitrocellulose membrane, before incubation with anti-CAII (1/2000) or anti-CAIII (1/1000) affinity-purified antibodies. The anti-CAIII antibodies do not detect any signal in the *Car3*$^{-/-}$ kidneys, whereas type II CA is detected with anti-CAII antibodies in both *Car3*$^{+/+}$ and *Car3*$^{-/-}$ samples. Loading control was performed after membrane stripping and incubation with monoclonal antibodies anti-β-actin (1/10 000). (**d**) Differential electrophoretic mobility of type II and III CA isozymes. A portion of 20 μg of cytosolic proteins from total kidneys (*n* = 2 wild-type mice) was separated by SDS-PAGE and blotted onto nitrocellulose membrane. Anti-CAII antibodies (1/2000) detected a unique band around ~29 kDa, whereas CAIII was identified by anti-CAIII antibodies (1/1000) at a slightly lower molecular weight (~27 kDa), without crossreactivity. (**e**, **f**) Representative immunoblotting for CAII and CAIII in *Clcn5*$^{Y/+}$ and *Clcn5*$^{Y/-}$ kidneys. A portion of 20 μg of cytosolic proteins was loaded in each lane. Blots were probed as in (**c**), and after stripping for β-actin (1/10 000). Densitometry analyses show that CAIII expression is ~4-fold higher in *Clcn5*$^{Y/-}$ kidneys than in controls (385 ± 43% of *Clcn5*$^{Y/+}$, *n* = 4 pairs of mice), whereas CAII abundance is unchanged (*$P < 0.05$).

## Upregulation of CAIII in human Dent's disease kidney samples

We investigated CAIII expression in two kidney cortex samples from the end-stage kidney of a patient with Dent's disease owing to the G506E mutation of *CLCN5*.[3] CAIII was upregulated at both mRNA and protein levels in these samples vs four end-stage kidney samples taken as controls (Figure 7a and c). Real-time RT-PCR studies also showed an induction of PCNA and thioredoxin expression in Dent kidney samples (Figure 7b). Despite tissue damage due to end-stage renal disease, the expression of CAIII could be located in PT cells, identified by co-staining with aquaporin-1 (Figure 7d). CAII was also apparently upregulated in Dent kidney samples, potentially related to metabolic acidosis. The CAII induction was not observed in mice lacking ClC-5 (Figure 3), which have no renal failure.[7] Although restricted to a single human kidney, these results correlate with the detection of CAIII in the urine of three other

patients with Dent's disease and normal renal function (Figure 4b). They support the hypothesis that the loss of ClC-5 in the kidney is associated with proliferation, protection against oxidative damage, and induction of CAIII in PT cells.

## Expression of CAIII mRNA in distinct mouse models of PT dysfunction

To clarify whether CAIII induction was specifically caused by ClC-5 inactivation or participated in a common cellular response to PT dysfunction, CAIII mRNA expression was investigated in two additional mouse models of renal Fanconi syndrome, namely, the megalin- and cystinosin-deficient mice. These models can be distinguished from each other by the severity of PT defects.[10,15] The expression of CAIII mRNA was significantly increased in the kidneys of mice lacking megalin (262 ± 22% of WT level, *n* = 3), whereas no changes were observed in the *Ctns* KO samples. Moreover,
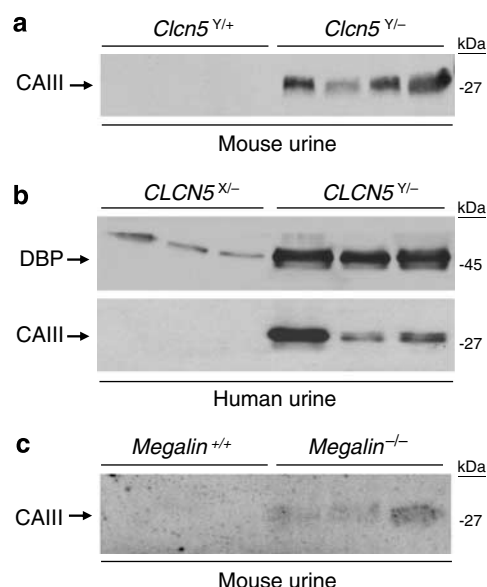
**Figure 4 | Urinary excretion of CAIII.** (**a**) Urine samples from $Clcn5^{Y/+}$ and $Clcn5^{Y/-}$ mice ($n = 4$ pairs of mice) were loaded on 14% PAGE, blotted onto nitrocellulose, and incubated with anti-CAIII antibodies (1/1000). Loading volume was normalized for urine creatinine concentration. CAIII is exclusively detected in $Clcn5^{Y/-}$ mouse urine. (**b**) Urine samples from three patients with Dent's disease and their carrier mothers were loaded on 14% PAGE, blotted onto nitrocellulose, and incubated with anti-DBP (1/1000) and anti-CAIII antibodies (1/1000). The LMW protein, DBP, is barely detected in carriers and excreted in large amounts in patients. CAIII is only detected in patients with Dent's disease. Loading volume was normalized for urine creatinine concentration. (**c**) Urine samples from $Lrp2^{+/+}$ and $Lrp2^{-/-}$ (megalin) mice ($n = 3$ pairs of mice) were loaded, according to creatinine concentration, on 14% PAGE, blotted onto nitrocellulose, and incubated with anti-CAIII antibodies (1/1000). CAIII is specifically detected in megalin-deficient mouse urine.

immunoblotting analyses detected a specific excretion of CAIII in the urine of mice lacking megalin (Figure 4c).

**Induction of CAIII expression in PT cells exposed to $H_2O_2$**

The HK-2 cell line is a well-established model for normal human PT cells.[16] Exposure of HK-2 cells to $H_2O_2$ 1 mM induced a significant increase in CAIII mRNA expression as early as 3 h postincubation, with a maximal level observed at 6 h. Immunoblotting analyses showed an early and stable induction of CAIII from 6 h postincubation with $H_2O_2$ (Figure 8). Similarly, exposure of OK cells to $H_2O_2$ 0.3 mM was associated with an increased expression of CAIII from 6 h postincubation (data not shown). These data demonstrate that PT cells rapidly increase their endogenous expression of CAIII in response to oxidative conditions.

**DISCUSSION**

We show here that the functional loss of ClC-5, taken as a paradigm of inherited PT dysfunction in mouse and man, is associated with higher cell turnover and increased cellular response to oxidant damage, as well as a major upregulation of CAIII, a CA isoform with no established role in the kidney.

Studies in cultured PT cells suggest that the induction of CAIII may be part of a cellular response to oxidative damage.

Owing to their intense reabsorptive activity involving active transport processes, the epithelial cells lining the PT are particularly vulnerable to injury. However, in contrast to the brain and heart, the PT cells can recover from an ischemic or toxic insult. After cell death by necrosis and apoptosis, the surviving cells dedifferentiate and proliferate to eventually replace the injured cells and restore tubular integrity.[17] Our studies reveal that a similar process occurs as a response to a chronic injury, that is, inherited renal Fanconi syndrome in mouse and man. The proliferative activity of PT cells, assessed by using antibodies to cell proliferation-associated nuclear proteins PCNA and KI-67, was almost fourfold increased, with the involvement of the $G_1$ cell cycle kinase being suggested by the upregulated cyclin E. Furthermore, PT cells underwent dedifferentiation, as indicated by the expression of osteopontin and the mesodermal marker CAIII (see below). These modifications occurred at a time when no visible alterations in PT cell morphology or renal failure were observed in ClC-5 KO mice,[7] and neither was there any change in the apoptotic rate.

The increased production of superoxide anion and the induction of type I superoxide dismutase and thioredoxin point to increased oxidative stress and solicitation of cell oxidative defenses in ClC-5 KO kidneys. Thioredoxin was also increased in a human kidney lacking functional ClC-5. Oxidative stress has also been documented in PT lesions induced by nephrotoxic compounds, such as cisplatin and heavy metals,[18,19] as well as in PT cells derived from patients with a renal Fanconi syndrome due to cystinosis.[11] These disorders have in common an alteration of the receptor-mediated endocytic uptake of albumin and LMW proteins, and the possibility of a link between oxidative stress and defective endocytosis could be raised. The endocytic defect caused by the loss of ClC-5 is reflected *in vivo* by a selective depletion of megalin (and its partner cubilin) from the brush border in the absence of morphological lesion.[6,8] Recently, Guggino et al.[20] suggested that megalin could act as a sensor of albumin and that a decrease in its plasma membrane expression could reduce protein kinase B activity and alter the survival pathway involving phosphorylation of Bad in cultured PT cells. The generalized trafficking defect in PT cells lacking ClC-5[8] could also impair the translocation/ activation of protein kinase B, further reducing defense against cytotoxicity. Furthermore, albumin is known to exert a potent survival activity in mouse PT cells, most likely through scavenging of reactive oxygen species,[21] so that a reduced capacity of albumin uptake may be deleterious. In contrast, excessive albumin endocytosis also promotes $H_2O_2$ generation in PT cells.[22] Thus, the link between oxidative stress and defective endocytosis remains speculative, and the two events could independently reflect the multiple changes induced by the loss of ClC-5 in PT cells.

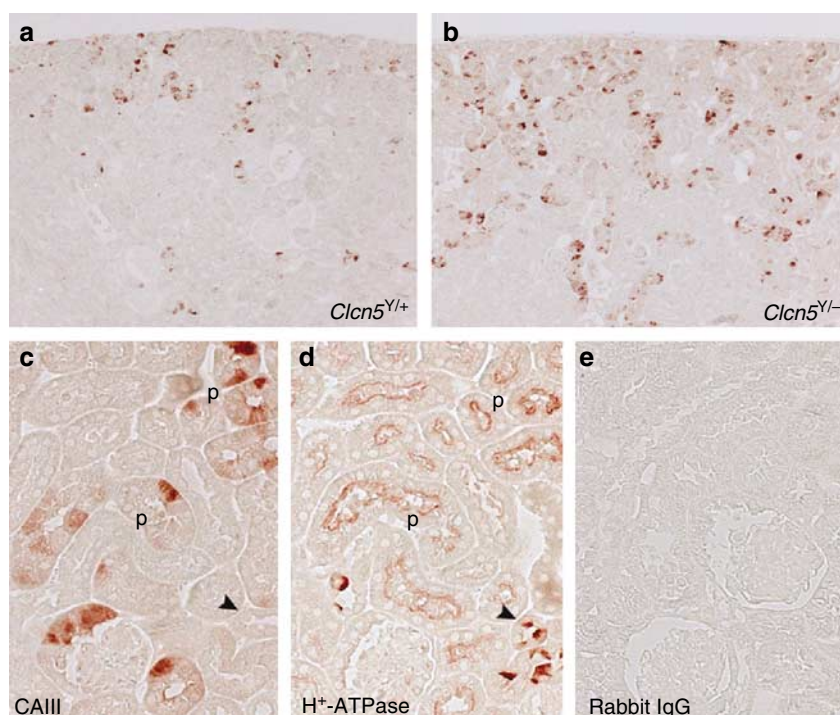At least 15 different CA isoforms with 11 catalytically active isozymes have been described in mammals, with

**Figure 5 | Segmental distribution of CAIII in mouse kidney.** Immunostaining for CAIII (**a–c**), V-ATPase E1 subunit (**d**) in *Clcn5*[Y/+] (**a, c–e**), and *Clcn5*[Y/−] (**b**). (**c, d**) are serial sections (p, proximal tubule). In mouse control kidney, CAIII is present in some tubules in the outer cortex (**a**). In *Clcn5*[Y/−] kidney, CAIII distribution includes both outer and inner cortices, with a ∼4-fold increased number of CAIII-positive cells (**b**). At higher magnification, CAIII is located in a subset of PT cells (**c**), identified by co-staining for the V-ATPase (**d**). The α-type intercalated cells of the collecting duct, which apically express the V-ATPase, are strictly negative for CAIII (**c, d**, arrowheads). No signal is detected after incubation with non-immune rabbit IgG (**e**). Bars = 100 μm (**a, b**); 50 μm (**c–e**).

distinct kinetic properties and tissue distribution.[12,23,24] The cytosolic type II and membrane-bound type IV represent the two major CA isoforms in the kidney, located in PT cells, where they participate in $H^+$ secretion, $HCO_3^-$ reabsorption, and NaCl homeostasis. CAII is also present in the intercalated cells of the collecting duct, where it ensures net urinary acidification. Two other CA isozymes (CAXIII and CAXIV) have been located in the mouse kidney, but their specific role remains unknown.[12] The cytosolic CAIII isoform is characterized by its resistance to sulfonamide inhibitors and its very low $CO_2$ hydration ability (∼2% of CAII activity) due to specific residues in the active site.[24,25] CAIII is abundantly expressed in the cytosol of skeletal muscle cells, adipocytes, and hepatocytes.[26] Trace amounts of CAIII have been previously identified by radioimmunoassay in the rat kidney,[27] but no role for this isoform has ever been mentioned.[12]

CAIII is known to function in an oxidizing environment,[28] which is relevant when considering the oxidative stress evidenced in mouse and human PT cells. Two reactive sulfhydryl groups of CAIII are rapidly *S*-thiolated by glutathione, after exposure to oxidative conditions, and dethiolated by glutaredoxin- and thioredoxin-like reactions.[29] CAIII may also play a protective role against $H_2O_2$-induced apoptosis, as NIH/3T3 cells overexpressing CAIII grow faster and are more resistant to cytotoxic concentrations of $H_2O_2$ than control cells.[30] It has been suggested that CAIII

functions as percarbonic acid anhydrase, which would mediate $H_2O_2 + CO_2 \leftrightarrow H_2CO_4$ detoxification.[26] The possibility that CAIII may function as an oxyradical scavenger in PT cells exposed to oxidative stress is supported by our studies in HK-2 and OK cells exposed to $H_2O_2$. Further studies should take advantage of the *Car3* KO mice[26] to verify whether this role can be established *in vivo*.

What could be the mechanism of CAIII induction in PT cells? Androgens regulate CAIII expression in the liver,[31] but we did not observe gender-dependent changes in CAIII mRNA expression in the kidney (data not shown). Thyroidectomy is known to increase CAIII concentration in rat muscle,[32] which could be relevant, as ClC-5 is involved in thyroid endocytosis.[33] However, ClC-5 KO mice develop a euthyroid goiter, without alterations in circulating T4 and thyroid-stimulating hormone levels.[33] Specific transcription factors may also regulate the transcription of CAIII in PT cells. For instance, *in silico* analyses revealed several potential hepatocyte nuclear factor 1 (HNF1) binding sites in the promoter of the *Car3* gene, and mice lacking HNF1α are characterized by a decreased renal expression of CAIII (F Jouret *et al.*, unpublished observations).

The selective detection of CAIII in urine samples of mice and patients lacking ClC-5 and other models of PT dysfunction suggests that it may represent a useful biomarker of renal Fanconi syndrome. As compared with traditional markers, such as LMW proteins (for example,
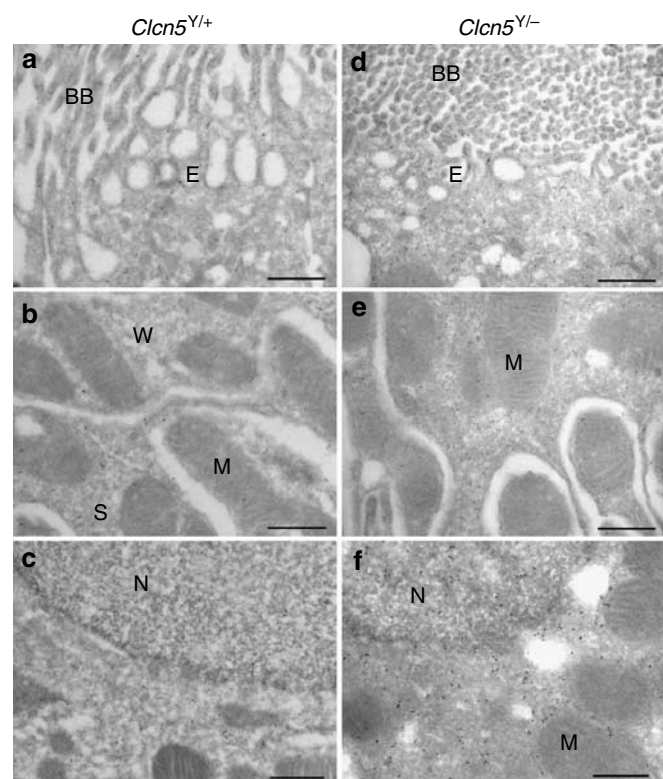
**Figure 6 | Subcellular distribution of CAIII in Clcn5$^{Y/+}$ and Clcn5$^{Y/-}$ kidneys.** EM immunocytochemistry for CAIII on ultrathin cryosections from renal cortex of Clcn5$^{Y/+}$ (a–c) and Clcn5$^{Y/-}$ mice (d–f). Labeling appears stronger in the Clcn5$^{Y/-}$ samples than in controls. The labeling is mainly cytosolic, extending to the apical brush border (BB) microvilli (a, d). Nuclei (N) are also labeled (c, f), and a possible endosomal labeling (E in a, d) cannot be excluded. The very low signal in mitochondria (M) was considered to be background. W and S in (b) denote weakly and strongly labeled neighbor cells (compared with Figure 5). Bars = 0.5 μm.

β2-microglobulin), which are produced outside the kidney, filtered but not reabsorbed owing to defective PT endocytosis, or PT cell components (such as N-acetyl-β-glucosaminidase) that appear in the urine in case of structural alterations, CAIII in the urine may directly reflect a state of cellular dysfunction, without changes in renal function or morphology. Furthermore, the upregulation of CAIII is organ- and segment-specific, and it is clearly conserved in mouse and man. Considering that CAIII is an early mesodermal marker,[34] it may reflect cell dedifferentiation along with other genes encoding growth and transcription factors that recapitulate the expression pattern seen during nephrogenesis.[17] Further investigations are necessary to substantiate the role of CAIII in other types of inherited or acquired PT dysfunction.

## MATERIALS AND METHODS
### Mouse models
Experiments were conducted on mice invalidated for Clcn5;[7] Lrp2 (megalin);[10] Ctns;[15] or Car3.[26] Mice lacking megalin in the kidney exhibit defective PT endocytosis, resulting in osteopathy and metabolic defects,[10] whereas the Ctns KO mice present no signs of proximal tubulopathy despite severe PT defects in infantile cystinosis.[15] The mice were housed in metabolic cages overnight with ad libitum access to food and drinking water. Urine was collected in ice-cold Complete protease inhibitors (Roche, Vilvoorde, Belgium), total volume was measured, and the samples immediately frozen and kept at −80 °C. An aliquot was used to measure the levels of creatinine by standard methods (Eastman Kodak Company, Rochester, NY, USA). All studies were in accordance with the National Institutes of Health (NIH) guidelines for the care and use of laboratory animals and approved by the Committee for Animal Rights of the UCL.

### Human samples
Two samples (outer cortex) from one end-stage kidney were obtained at the time of nephrectomy in a patient with Dent's disease due to the G506E mutation in CLCN5.[3] Four cortical samples from end-stage kidneys (chronic interstitial nephritis) removed during renal transplantation were used as controls. The kidney samples were frozen in liquid nitrogen or fixed in 4% formaldehyde. We obtained urine samples (second morning miction) from three unrelated patients with Dent's disease harboring nonsense mutations (S203X, R637X, and R648X) in CLCN5 and from their asymptomatic carrier mothers. All patients (aged 7, 15, and 13 years, respectively) had LMW proteinuria and hypercalciuria but no renal failure. The use of these samples has been approved by the Ethical Review Board of the UCL.

### PT cell lines
The human kidney (HK-2) and opossum kidney (OK) cell lines were cultured as described.[16] After 24 h serum deprivation, subcultures of HK-2 (passage 12) and OK cells (passage 111) were treated with $H_2O_2$ (1 or 0.3 mM, respectively) for 1–14 h. Cell pellets were harvested and kept at –80 °C before mRNA and protein extraction.

### RNA extraction and double-strand cDNA synthesis
Total RNA was extracted using Trizol (Invitrogen, Merelbeke, Belgium). For AFLP, poly(A)+ RNA was prepared from total RNA using Dynabeads Oligo(dT)$_{25}$ (Invitrogen). First-strand cDNA was synthesized from 500 ng of poly(A)+ RNA using SuperScript II RNase H⁻ Reverse Transcriptase (Invitrogen). Double-strand cDNA was synthesized using T4 DNA Polymerase and purified using QIAquick Extraction Kit (Qiagen, Venlo, The Netherlands).

### AFLP reactions
The AFLP protocol was performed as described previously.[35] cDNA samples were digested with EcoRI and MseI (Fermentas, Vilnius, Lithuania) and ligated to EcoRI and MseI double-strand adapters (Supplementary Table S1) for 2 h at 20 °C. The restriction fragments with ligated adapters were diluted (10×) with TE buffer (100 mM Tris-HCl, 10 mM EDTA, pH 8.0) and used as a template for the pre-amplification reaction, which was performed for 20 cycles (94 °C, 30 s; 56 °C, 1 min; 72 °C, 1 min) using Eco-P0 and Mse-P0 primers. The product was diluted (10×) with TE buffer, and 5 μl was used for selective amplification as follows: 33 cycles including 9 touchdown cycles comprising a decrease of the annealing temperature from 65 to 56 °C, which was maintained for 24 cycles. Twelve primer combinations were used for selective amplification (Eco-PAA and Mse-PAA or Mse-PAC or Mse-PAT; Eco-PAC and Mse-PAA or
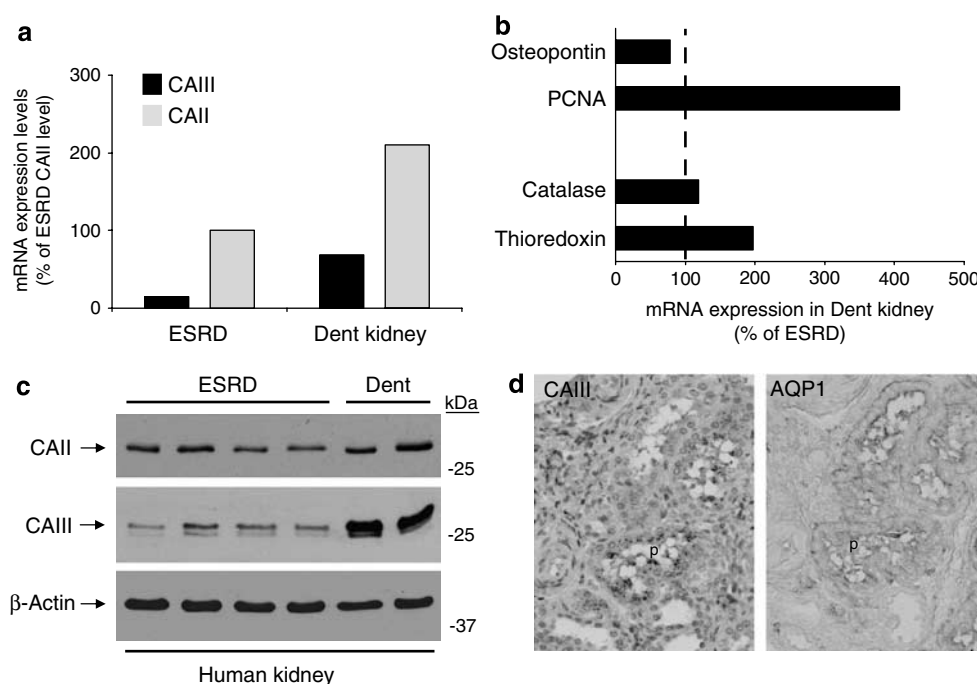
**Figure 7 | Expression and distribution of CAIII in human Dent's disease kidney. (a, b)** Real-time RT-PCR quantification of mRNA expression of type III and II CA isozymes (**a**), osteopontin, PCNA, catalase, and thioredoxin (**b**) in two cortical samples from one end-stage kidney from a patient with Dent's disease vs four cortical samples obtained in end-stage kidneys of patients with an unrelated pathology (ESRD). The mRNA levels were adjusted to GAPDH and quantified using the formula: ratio $= 2^{-\Delta\Delta C_t}$. The CAIII mRNA expression is $\sim$4-fold higher in Dent's disease samples vs ESRD controls, and associated with increased PCNA and thioredoxin mRNA levels. Note that CAII mRNA is also increased in the kidney samples of the patient with Dent's disease. (**c**) Representative immunoblotting for CAIII and CAII isoforms in the human kidney samples described above in (**a**). The blots were probed with antibodies against CAIII (1/1000) or CAII (1/2000), and after stripping, β-actin (1/10 000). A strong CAIII expression is observed in Dent's disease kidney. (**d**) Immunostaining for CAIII (left) and aquaporin-1 (right) in human Dent's disease kidney. CAIII is located diffusely in some PT cells (p), identified by staining for AQP1.

*Mse*-PAC or *Mse*-PAT; *Eco*-PAG and *Mse*-PAA or *Mse*-PAC or *Mse*-PAT; *Eco*-PAT and *Mse*-PAA or *Mse*-PAC or *Mse*-PAT) using an iCycler Thermal Cycler (Bio-Rad, Nazareth, Belgium). The amplification products were denatured and separated on sequencing gels (6% polyacrylamide, 6 M urea) that were then dried and exposed to Kodak BioMax film (Amersham Biosciences, Buckinghamshire, UK). The bands of interest were removed from the gel and recovered by PCR. Reamplified cDNAs were visualized on a 1.5% (w/v) agarose gel, subcloned into pGEM-T easy vector (Promega, Leiden, The Netherlands), and sequenced (Genome Express, Meylan, France). Each re-amplified AFLP fragment was analyzed using the BLAST sequence alignment program (http://www.ncbi.nlm.nih.gov/BLAST/).

**Real-time RT-PCR**
Total RNA was treated with DNase I (Invitrogen) and reverse-transcribed using SuperScript III RNase H⁻ Reverse Transcriptase (Invitrogen). Changes in mRNA expression levels were determined by real-time RT-PCR (iCycler iQ System; Bio-Rad) using SYBR Green I (Invitrogen).[36] Specific primers were designed using Beacon Primer Designer 2.0 (Premier Biosoft International, Palo Alto, CA, USA) (Supplementary Table S2). The PCR products were sequenced by Genome Express. The efficiency of each set of primers was determined by dilution curves (Supplementary Table S2), and the $C_t$ differences between the reference (GAPDH, glyceraldehyde-3-phosphate dehydrogenase) and target genes were calculated for

each sample of each genotype. The formula used to quantify the relative changes in target over GAPDH mRNAs between the two groups is derived from the $2^{-\Delta\Delta C_t}$ formula as described by Pfaffl.[37]

**Antibodies**
The following antibodies were used: monoclonal antibodies against CAIII (Spectral, Toronto, ON, Canada); V-ATPase E1 subunit (a gift of Dr S Gluck, University of California, San Francisco, CA, USA); PCNA (Dako, Heverlee, Belgium); β-actin (Sigma, St Louis, MO, USA); and Ki67 antigen (Dako); and polyclonal antibodies against CAIII;[13] aquaporin-1 (Chemicon, Temecula, CA, USA); CAII (Serotec, Oxford, UK); and vitamin D-binding protein (DBP) (Dako). The specificity of anti-CAIII antibodies has been documented against purified CAI and CAII[13] and in reference tissue samples, including *Car3* KO kidneys[26] (Figure 3c), red blood cell ghosts, and epididymis (data not shown).

**Protein extraction and Immunoblotting**
Cytosolic proteins were extracted from kidney samples as described.[7,36] Cell lysates were obtained by solubilizing frozen pellets in lysis buffer containing Complete Mini (Roche), followed by sonication and centrifugation at 16 000 g for 1 min at 4 °C. Protein concentrations were determined using bicinchoninic acid protein assay (Pierce, Aalst, Belgium). Tissue and urine samples were thawed on ice, normalized for protein or creatinine levels, diluted in Laemmli buffer, separated on sodium dodecyl
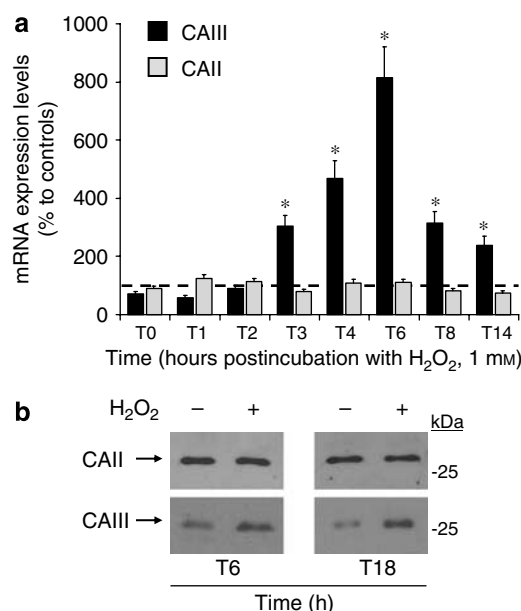
**Figure 8 | Time course of CAIII mRNA expression in HK-2 cells after $H_2O_2$ exposure.** (a) Real-time RT-PCR analyses of CAIII and CAII mRNA abundance in HK-2 cells after various periods of exposure to $H_2O_2$ (1 mM). Quantifications were performed after adjustment to GAPDH mRNA levels and in comparison to time-matched controls. The expression of CAIII mRNA significantly increases from 3 h after $H_2O_2$ treatment, whereas no changes are observed in CAII. Values are presented as means ± s.d.; *$P < 0.05$. (b) Representative immunoblotting for CAIII and CAII expression in HK-2 cells at various time points after exposure to $H_2O_2$ (1 mm). A portion of 30 μg proteins was loaded, blotted onto nitrocellulose membrane, and incubated with antibodies anti-CAIII (1/1000) or anti-CAII (1/2000). In comparison to non-treated cells, $H_2O_2$-treated HK-2 cells show an increased expression of CAIII from 6 h post-treatment, with no changes in CAII expression.

sulfate-polyacrylamide gel electrophoresis ($10 \times 7$ cm, 14% gels) in reducing conditions, and blotted onto nitrocellulose as described.[36] Densitometry analysis was performed with a Canon CanoScan 8000F using the NIH Image V1.60 software.

### Immunostaining and immunogold labeling

Kidney samples were fixed in 4% formaldehyde in 0.1 M phosphate buffer, pH 7.4, and embedded in paraffin. Immunostaining was performed on 6 μm sections using avidin–biotin peroxidase (Vectastain Elite; Vector Laboratories, Labconsult, Brussels, Belgium) and aminoethylcarbazole.[37] Controls without primary antibody or with non-immune IgG (Vector Laboratories) were negative. Counting of PCNA-, Ki67-, and CAIII-positive PT cells was blindly performed on five different cortex areas in four pairs of $Clcn5^{Y/-}$ vs $Clcn5^{Y/+}$ kidneys. For immunogold labeling, kidneys were fixed by retrograde perfusion with 2% formaldehyde in 0.1 M sodium cacodylate buffer, pH 7.2, and 70–90 nm cryosections were obtained with an FCS Reichert Ultracut S cryo-ultramicrotome as described.[38] Sections were incubated with rabbit anti-CAIII at 4 °C overnight, followed by incubation for 1 h with 10 nM goat anti-rabbit gold particles (BioCell, Cardiff, UK). The cryosections were embedded in methylcellulose containing 0.3% uranyl acetate and studied in a Philips CM100 electron microscope. Controls with secondary antibody alone or with nonspecific rabbit serum were negative.

### Detection of superoxide anion ($O_2^{\bullet-}$) generation

The *in situ* production of $O_2^{\bullet-}$ in kidney sections was assessed using the hydroethidine fluorescence method and detection of fluorescent ethidium bromide as described.[39] Briefly, kidney cryosections were incubated with 50 μl of $2 \times 10^{-6}$ M HB solution (Invitrogen) in water at 37 °C for 30 min in a light-protected and humidified chamber. Red fluorescence from hydroethidine-treated samples was measured during 5 ms using the software KS400 (Zeiss, Zaventem, Belgium) through a Zeiss Axiovert S100 microscope equipped with an Axiocam camera.

### Statistics

Results are expressed as means ± s.d. Comparisons between groups were made by Student's unpaired *t*-tests. The significance level was set at $P < 0.05$.

### SUPPLEMENTARY MATERIAL

**Table 1.** Nucleotide sequence of adapters and primers used for AFLP reactions.
**Table 2.** Primers used for real-time RT-PCR.

### REFERENCES

1. Christensen EI, Birn H. Megalin and cubilin: multifunctional endocytic receptors. *Nat Rev Mol Cell Biol* 2002; **3**: 256–266.
2. Marshansky V, Ausiello DA, Brown D. Physiological importance of endosomal acidification: potential role in proximal tubulopathies. *Curr Opin Nephrol Hypertens* 2002; **11**: 527–537.
3. Lloyd SE, Pearce SH, Fisher SE *et al.* A common molecular basis for three inherited kidney stone diseases. *Nature* 1996; **379**: 445-449.
4. Devuyst O, Christie PT, Courtoy PJ *et al.* Intra-renal and subcellular distribution of the human chloride channel CLC-5, reveals a pathophysiological basis for Dent's disease. *Hum Mol Genet* 1999; **8**: 247–257.
5. Moulin P, Igarashi T, Van der Smissen P *et al.* Altered polarity and expression of H$^+$-ATPase without ultrastructural changes in kidneys of Dent's disease patients. *Kidney Int* 2003; **63**: 1285–1295.
6. Piwon N, Gunther W, Schwake M *et al.* ClC-5 Cl$^-$—channel disruption impairs endocytosis in a mouse model for Dent's disease. *Nature* 2000; **408**: 369–373.
7. Wang SS, Devuyst O, Courtoy PJ *et al.* Mice lacking renal chloride channel CLC-5, are a model for Dent's disease, a nephrolithiasis disorder associated with defective receptor-mediated endocytosis. *Hum Mol Genet* 2000; **9**: 2937–2945.
8. Christensen EI, Devuyst O, Dom G *et al.* Loss of chloride channel ClC-5 impairs endocytosis by defective trafficking of megalin and cubilin in kidney proximal tubules. *Proc Natl Acad Sci USA* 2003; **100**: 8472–8477.
9. Aminoff M, Carter JE, Chadwick RB *et al.* Mutations in CUBN, encoding the intrinsic factor-vitamin B12 receptor, cubilin, cause hereditary megaloblastic anaemia. *Nat Genet* 1999; **21**: 309–313.
10. Leheste JR, Melsen F, Wellner M *et al.* Hypocalcemia and osteopathy in mice with kidney-specific megalin gene defect. *FASEB J* 2003; **17**: 247–249.

11. Wilmer MJ, de Graaf-Hess A, Blom HJ *et al*. Elevated oxidized glutathione in cystinotic proximal tubular epithelial cells. *Biochem Biophys Res Commun* 2005; **337**: 610–614.

12. Purkerson JM, Schwartz GJ. The role of carbonic anhydrases in renal physiology. *Kidney Int* 2007; **71**: 103–115.

13. Nishita T, Matsuura K, Ichihara N *et al*. Isolation and measurement of carbonic anhydrase isoenzyme III in plasma, sera, and tissues of dogs. *Am J Vet Res* 2002; **63**: 229–235.

14. Tweedie S, Edwards Y. Mouse carbonic anhydrase III: nucleotide sequence and expression studies. *Biochem Genet* 1989; **27**: 17–30.

15. Cherqui S, Sevin C, Hamard G *et al*. Intralysosomal cystine accumulation in mice lacking cystinosin, the protein defective in cystinosis. *Mol Cell Biol* 2002; **22**: 7622–7632.

16. Ryan MJ, Johnson G, Kirk J *et al*. HK-2: an immortalized proximal tubule epithelial cell line from normal adult human kidney. *Kidney Int* 1994; **45**: 48–57.

17. Bonventre JV. Dedifferentiation and proliferation of surviving epithelial cells in acute renal failure. *J Am Sol Nephrol* 2003; **14**: S55–S61.

18. Kawai Y, Nakao T, Kunimura N *et al*. Relationship of intracellular calcium and oxygen radicals to cisplatin-related renal cell injury. *J Pharmacol Sci* 2006; **100**: 65–72.

19. Sabolic I. Common mechanisms in nephropathy induced by toxic metals. *Nephron Physiol* 2006; **104**: 107–114.

20. Caruso-Neves C, Pinheiro AACS, Cai H *et al*. PKB and megalin determine the survival or death of renal proximal tubule cells. *Proc Natl Acad Sci USA* 2006; **103**: 18810–18815.

21. Iglesias J, Abernethy VE, Wang Z *et al*. Albumin is a major serum survival factor for renal tubular cells and macrophages through scavenging of ROS. *Am J Physiol Renal Physiol* 1999; **277**: F711–F722.

22. Imai E, Nakajima H, Kaimori JY. Albumin turns on a vicious spiral of oxidative stress in renal proximal tubules. *Kidney Int* 2004; **66**: 2085–2087.

23. Sly WS, Hu PY. Human carbonic anhydrases and carbonic anhydrase deficiencies. *Annu Rev Biochem* 1995; **64**: 375–401.

24. Lindskog S. Structure and mechanism of carbonic anhydrase. *Pharmacol Ther* 1997; **74**: 1–20.

25. Jewell DA, Tu CK, Paranawithana SR *et al*. Enhancement of the catalytic properties of human carbonic anhydrase III by site-directed mutagenesis. *Biochemistry* 1991; **30**: 1484–1490.

26. Kim G, Lee TH, Wetzel P *et al*. Carbonic anhydrase III is not required in the mouse for normal growth, development, and life span. *Mol Cell Biol* 2004; **24**: 9942–9947.

27. Shiels A, Jeffery S, Wilson C, Carter N. Radioimmunoassay of carbonic anhydrase III in rat tissues. *Biochem J* 1984; **218**: 281–284.

28. Cabiscol E, Levine RL. Carbonic anhydrase III. Oxidative modification *in vivo* and loss of phosphatase activity during aging. *J Biol Chem* 1995; **270**: 14742–14747.

29. Chai YC, Jung CH, Lii CK *et al*. Identification of an abundant *S*-thiolated rat liver protein as carbonic anhydrase III; characterization of *S*-thiolation and dethiolation reactions. *Arc Biochem Biophys* 1991; **284**: 270–288.

30. Raisanen SR, Lehenkari P, Tasanen M *et al*. Carbonic anhydrase III protects cells from hydrogen peroxide-induced apoptosis. *FASEB J* 1999; **13**: 513–522.

31. Carter N, Lonnerholm G, Meyerson B *et al*. Androgen-linked control of carbonic anhydrase III expression occurs in rat perivenous hepatocytes; an immunocytochemical study. *Ups J Med Sci* 2001; **106**: 67–76.

32. Jeffery S, Carter ND, Smith A. Thyroidectomy significantly alters carbonic anhydrase III concentration and fiber distribution in rat muscle. *J Histochem Cytochem* 1987; **35**: 663–668.

33. van den Hove M-F, Croizet-Berger K, Jouret F *et al*. The loss of the chloride channel, ClC-5, delays apical iodide efflux and induces a euthyroid goiter in the mouse thyroid gland. *Endocrinology* 2006; **147**: 1287–1296.

34. Lyons GE, Buckingham ME, Tweedie S *et al*. Carbonic anhydrase III, an early mesodermal marker, is expressed in embryonic mouse skeletal muscle and notochord. *Development* 1991; **111**: 233–244.

35. Vos P, Hogers R, Bleeker M *et al*. AFLP: a new technique for DNA fingerprinting. *Nucleic Acids Res* 1995; **23**: 4407–4414.

36. Jouret F, Bernard A, Hermans C *et al*. Cystic fibrosis is associated with a defect in apical receptor-mediated endocytosis in mouse and human kidney. *J Am Soc Nephrol* 2007; **18**: 707–718.

37. Pfaffl MW. A new mathematical model for relative quantification in real-time RT-PCR. *Nucleic Acids Res* 2001; **29**: 2002–2007.

38. Christensen EI, Nielsen S, Moestrup SK *et al*. Segmental distribution of the endocytosis receptor gp330 in renal proximal tubules. *Eur J Cell Biol* 1995; **66**: 349–364.

39. Piech A, Dessy C, Havaux X *et al*. Differential regulation of nitric oxide synthases and their allosteric regulators in heart and vessels of hypertensive rats. *Cardiovasc Res* 2003; **57**: 456–467.